

Rapid Commun. Mass Spectrom. 2013, 27, 187–199
(wileyonlinelibrary.com) DOI: 10.1002/rcm.6429

Identification of low molecular weight organic acids by ion chromatography/hybrid quadrupole time-of-flight mass spectrometry during Uniblu-A ozonation

Apollonia Amorisco, Vito Locaputo, Carlo Pastore and Giuseppe Mascolo*

Istituto di Ricerca Sulle Acque, Consiglio Nazionale delle Ricerche, Viale F. De Blasio 5, 70132 Bari, Italy

RATIONALE: The balance of organic nitrogen and sulfur during ozonation of organic pollutants often shows a lack of complete mineralization. It follows that polar and ionic by-products are likely to be present that are difficult to identify by liquid chromatography/mass spectrometry (LC/MS).

METHODS: The structural elucidation of low molecular weight organic acids arising from Uniblu-OH ozonation has been investigated by ion chromatography/electrospray tandem mass spectrometry (IC/ESI-MS/MS) employing a quadrupole time-of-flight mass spectrometer. Unequivocal elemental composition of the by-products was determined by a combination of mass accuracy and high spectral accuracy.

RESULTS: The employed identification strategy was demonstrated to be a powerful method of unequivocally assigning a single chemical composition to each identified compound. The exact mass measurements of $[M-H]^-$ ions allowed the elemental formulae and related structures of eighteen by-products to be determined confidently. The main degradation pathways were found to be decarboxylation and oxidation. The experimental procedure allowed the identification of both nitrogen- and sulfur-containing organic acid by-products arising from Uniblu-OH ozonation.

CONCLUSIONS: The obtained results are of environmental relevance for the balance of organic nitrogen and sulfur during the ozonation of organic pollutants due to the lack of complete mineralization of the compounds containing these atoms. Copyright © 2012 John Wiley & Sons, Ltd.

It is known that the removal of organic pollutants during wastewater and drinking water treatment can be successfully achieved by powerful chemical methods, such as ozone treatment alone or ozone combined with UV or hydrogen peroxide.^[1] The latter methods are known as advanced oxidation processes (AOPs) and are based on the generation of hydroxyl radicals ($\cdot OH$), which, in turn, are able to oxidize contaminants in a non-selective manner.^[2–7] AOPs are not employed at high dosages due to the high operational costs. This leads, in addition to the complete removal of parent organic pollutants, to the formation of several degradation products, which may be more toxic than the parent compounds.^[8,9] It follows that the identification of the chemical structures of degradation products is a key issue for the environmental understanding of the investigated treatment process. As AOPs are oxidative processes, the resulting degradation by-products are more polar than the parent compounds, and liquid chromatography/electrospray ionization mass spectrometry (LC/ESI-MS), often employing accurate mass measurement, is a suitable technique for their analysis.^[10,11] The degradation products formed in the early stage of AOPs are transient compounds

and they are further degraded, leading to the formation of low molecular weight carbonyl compounds which, in turn, are finally degraded to low molecular weight organic acids. Previous investigation showed that during the ozonation of dyestuffs, low molecular weight carbonyl compounds and organic acids identified only on the basis of authentic standards failed to account for the total organic carbon present in the ozonated aqueous solution.^[12] It follows that other low molecular weight compounds are present that are not detectable in reversed-phase LC. Ion chromatography (IC) can, however, also be conveniently interfaced to ESI-MS and combined with accurate mass measurement, both in single and tandem MS, for the identification of unknown low molecular weight organic acids.

Such an approach was used herein to identify the final degradation product during the ozonation of hydrolyzed Uniblu-A (Uniblu-OH) at long contact times. Uniblu-A is a representative reactive dyestuff based on the anthraquinone structure used in cellulose fiber dyeing. Due to their fused aromatic structure these compounds are more resistant to biodegradation than azo-based ones.^[13] The recovery of residual dye from spent baths is not possible because the fixation reaction onto fibers leads to the formation of the hydrolyzed dyestuff. As the fixation rate is usually below 90% the resulting spent waters are of no further use and they should be disposed of properly. Therefore, the efficient removal of residual hydrolyzed dye from wastewater is of environmental relevance.

* Correspondence to: G. Mascolo, Istituto di Ricerca Sulle Acque, Consiglio Nazionale delle Ricerche, Viale F. De Blasio 5, 70132 Bari, Italy.
E-mail: giuseppe.mascolo@ba.irsra.cnr.it

It was previously shown that ozonation of Uniblu-OH led to the formation of intermediate by-products more polar than the parent compound.^[12] Their further degradation led to the formation of low molecular carbonyl compounds, aldehydes and ketones,^[14] which, in turn, as a result of extensive oxidation of the Uniblu-OH, disappeared leading probably to hydroxylated organic acids.

Several methods, e.g. gas chromatography (GC),^[15,16] capillary electrophoresis (CE),^[17,18] LC,^[19,20] and various kinds of ion chromatography, such as ion-exchange chromatography and ion-exclusion chromatography,^[21,22] are suitable for the analysis of polyhydroxy organic acids. In particular, ion chromatography with conductivity detection (IC-CD) has been employed in many applications.^[23–25]

The identification of final ozonation by-products should be possible by coupling an IC system, equipped with a membrane ion suppressor, and ESI-MS using accurate mass measurement, both in single and tandem MS, using quadrupole time-of-flight mass spectrometry (QqTOF-MS), although it is not always possible to differentiate isomers. In IC/ESI-MS a membrane ion suppressor is successfully used to minimize background spectral interferences and to enhance the $[M-H]^-$ ion signal. Therefore, it is possible to combine the advantages of the unique selectivity offered by IC with the specificity and structural elucidation capability of MS.^[26–29] IC/MS has previously been successfully used for the detection of inorganic and organic species at low detection limits.^[30,31] However, only a few studies have focused on its use for the analysis of low molecular mass mono- and dicarboxylic acids.^[32–34] Specifically, in IC/ESI-MS the use of a membrane ion suppressor has been proved to effectively remove sodium ions from the mobile phase that cause the formation in the MS interface of uncharged species (i.e. organic/inorganic anion with a sodium counter-ion). These neutral species reduce transfer efficiency from the atmospheric part of the interface to the vacuum region causing, in turn, a decrease in the MS detection sensitivity. Therefore, the ion suppressor makes it possible to combine the advantages of the unique selectivity offered by IC with the specificity and structural elucidation capability of MS.^[31,35,36]

The objective of this investigation was the identification of low molecular weight aliphatic carboxylic acids, formed as end products during the ozonation of hydrolysed Uniblu-A (Uniblu-OH). The assignment of chemical structures was made possible by combining high-resolution mass spectrometry data, obtained in single and in tandem MS mode, with the information contained in high-resolution mass spectra about the isotopic distribution of ions, defined as spectral accuracy.^[37,38] Several reports have focused on how isotope

pattern can be used as a tool to help identify unknowns on various mass spectrometer types. In this case the concept of spectral accuracy was employed to further enhance the formula determination using a high-resolution time-of-flight instrument.

EXPERIMENTAL

Chemicals

Uniblu-A (95% purity; Sigma-Aldrich, Milan, Italy) was used without further purification. Uniblu-OH was obtained by hydrolyzing an aqueous solution of Uniblu-A (500 mg/L) at pH 12 and 50 °C for 1 h (hydrolysis yield >90%),^[14] as shown in Scheme 1.

Water used for ion chromatography as well as for preparing all standard aqueous solutions (18.2 MΩcm, organic carbon content ≤4 μg/L) was obtained from a Milli-Q Gradient A-10 system (Millipore, Billerica, MA, USA). NaOH used for IC was from J.T. Baker (Deventer, The Netherlands). All other reagents were analytical grade and purchased from VWR (Milan, Italy) or Carlo Erba (Milan, Italy).

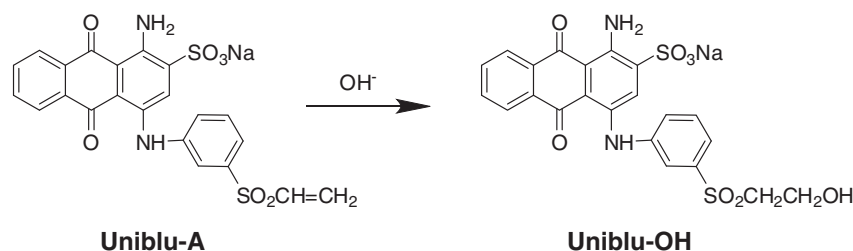
Ozonation experiments

Uniblu-OH aqueous solution (500 mL), after adjusting the pH to 7 by the addition of HCl, was placed into a Normag reactor (Hofheim am Taunus, Germany). Ozone was produced by a 502 ozonator (Fisher, Meckenheim, Germany) fed with oxygen. The oxygen/ozone mixture (flow rate of 1 L/min, 16 mg/L) was split to allow only 0.1 L/min to be bubbled into the Normag reactor. The ozone output was monitored before each experiment by determining (by titration with sodium thiosulfate) the amount of free iodine liberated from a potassium iodide solution. Samples (10 mL) were withdrawn from the reaction mixtures at scheduled times and the residual ozone was stripped from them by purging with air.

IC/ESI-QqTOFMS and IC/ESI-QqTOFMS/MS analysis

Data acquisition

Determinations were carried out by a GS50 chromatography system (Dionex-Thermo Fisher Scientific, Sunnyvale, CA, USA) equipped with an AS50 autosampler, an ED50 conductivity detector and an ASRS-ultra suppressor, operated at 100 mA in external water mode. Samples, injected via a 25 μL loop, were eluted at a flow rate of 0.5 mL/min through an analytical IonPac AS-11 column (250 mm × 2 mm; Dionex)



Scheme 1. Uniblu-A hydrolysis employed to obtain Uniblu-OH.

equipped with a IonPac AG-11 guard-column (50 mm × 2 mm) with the following gradient: from 10/0/90 (NaOH 5 mM/NaOH 100 mM/water), held for 2.5 min, to 100/0/0 in 3.5 min, then to 50/50/0 in 12 min, held for 5 min. The flow from the conductivity detector of the IC system was split 1:1, by means of a zero dead volume T-piece, to allow one-half to enter the interface of the mass spectrometer. The optimization of the ESI-MS interface was performed by using only the IonPac AG-11 guard column in isocratic mode (0/20/80 of NaOH 0.5 mM/NaOH 100 mM/water) at a flow rate of 0.5 mL/min. These analytical conditions were carefully chosen in order to elute all the organic acids within 2 min and, consequently, to run several injections during a MS acquisition for optimizing each ESI interface parameter. Ten μL of a standard solution of organic acids (1 mg/L) was injected through a 7125-Ti Rheodyne valve.

A QSTAR QqTOFMS/MS system (AB Sciex, Framingham, MA, USA) equipped with a TurboIonSpray source operated in negative ion mode was used throughout this work. High-purity nitrogen gas was used as both the curtain and the collision gas, while high-purity air was used as the nebulizer and auxiliary heated gas. The TurboIonSpray interface conditions were: nebulizer voltage, -4200 V ; declustering potential, -40 V ; focusing potential, -120 V ; nebulizer gas flow rate, 1 L/min; curtain gas flow rate, 0.66 L/min; and auxiliary gas (air) delivered by a turbo heated probe, flow rate 5.5 L/min at $450\text{ }^\circ\text{C}$. Accurate mass measurements (four decimal places) were carried out at a mass resolution higher than 5000 (full width at half maximum) by obtaining averaged spectra from chromatographic peaks and then recalibrating them using the $[\text{M}-\text{H}]^-$ ions of a five-acids mix injected post-column: $\text{C}_2\text{H}_3\text{O}_2^-$ at m/z 59.0139, C_2HO_3^- at m/z 72.9931, $\text{C}_2\text{H}_2\text{ClO}_2^-$ at m/z 92.9749, $\text{C}_8\text{H}_7\text{O}_3^-$ at m/z 151.0395 and $\text{C}_{10}\text{H}_{10}\text{O}_3\text{Cl}^-$ at m/z 213.0324 with its characteristic fragment ion at m/z 126.9956. The product ion mass measurements were carried out by fragmenting the target precursor $[\text{M}-\text{H}]^-$ ions at an optimized collision voltage (CV) and at a collision gas pressure of 4 mTorr. Each averaged spectrum was recalibrated using, as a lock mass, the precursor ion mass obtained in single MS mode. The collision energy (CE) was optimized for each compound in order to obtain, where possible, spectra showing acceptable signal-to-noise (S/N) ratios in the MS/MS spectra, with both the $[\text{M}-\text{H}]^-$ ion and the greatest number of product ions of high enough abundance for accurate mass determination.

Data analysis

All MS data handling was performed using Analyst QS software (AB Sciex). All mass spectral data acquired by QqTOFMS were exported as ASCII data and analyzed by sCLIPS (self Calibrated Line-shape Isotope Profile search) through Mass Works (version 2.0; Cerno Bioscience, Danbury, CT, USA). sCLIPS is a formula determination tool that performs a peak-shape-only calibration and matches calibrated experimental isotope pattern against possible theoretical ones using the spectral accuracy as discussed later. The mass tolerance for the sCLIPS searches was 10 ppm. The elemental number was restricted to include C, H, O, N, and S. The formula constraints were set by the software on the basis of chemical rules, i.e. $\text{C}, \text{H}, \text{O} \geq 1, \text{S} \geq 0, \text{and } \text{N} \geq 0 \text{ or } 1$, following the nitrogen rule. The number of double-bond

equivalents (DBEs) was set between -0.5 and 5.0 . The profile mass range, which determines the relative mass spectral range used for the isotope profile comparison and the spectral accuracy calculation, was set between -0.5 and 2.5 . The calibration range was centered to the approximate m/z value of the monoisotopic peak and was 1 m/z unit wide. The spectral accuracy was calculated as $(1 - \text{RMSE}) \times 100$ where RMSE is the fit error between the calibrated and theoretical spectra.

RESULTS AND DISCUSSION

A detailed screening of the degradation products formed during Uniblu-OH ozonation was carried out. The intermediate degradation products were identified employing conventional reversed-phase HPLC/MS.^[12] At reaction times longer than 15 min such compounds disappeared completely. Several low molecular weight aldehydes and ketones were identified employing derivatization with 2,4-dinitrophenyl hydrazine (DNPH).^[14] Once again, these compounds disappeared after time but the total organic carbon content of the aqueous solution did not reduce consistently. This suggested that a number of very polar degradation products had been formed as a result of extensive oxidation. Such compounds are likely to be low molecular weight organic acids. This is also consistent with the acidic pH (3.7) of the reaction mixture at longer ozonation times. Ozonated samples were also analyzed for organic acids on the basis of authentic standards (oxalic and formic acids).^[12] Preliminary evidence on other minor peaks, not identified for lack of authentic standards, suggested the presence of several novel acids. In addition, on the basis of the low extent of both nitrogen and sulfur mineralization during ozonation, it was reasonable to assume the presence of very polar sulfur- and nitrogen-containing by-products, presumably ionic, and therefore not detectable by reverse phase HPLC.

IC interfaced to ESI-QqTOFMS was employed for the identification of such final by-products allowing 18 unknown by-products to be identified on the basis of accurate mass measurements of the $[\text{M}-\text{H}]^-$ ions (Table 1). It should be noted that the mass-measured $[\text{M}-\text{H}]^-$ ions reported in Table 1 often do not have a single unequivocally assigned elemental composition due to the employed QqTOFMS instrumentation (accurate mass error 5 ppm). The number of candidates could be reduced by limiting the possible elements as well as by applying other chemical constraints. In the present investigation it was only possible to set $-0.5 \leq \text{DBE} \leq 5.0$ and to include C, H, N, O and S for elemental composition, consistent with Uniblu-OH ozonation at a long reaction time. In order for the elemental composition of each by-product to be unequivocally assigned, spectral accuracy was also employed. Spectral accuracy is the measure of similarity between the entire ion isotope pattern spectrum and the theoretical one. Several papers about the calculation of theoretical isotope distributions and on convolution of a peak shape function have been published.^[39–41] The results obtained using spectral accuracy are also listed in Table 1. It should be noted that, despite the limited instrumental mass accuracy, the employment of spectral accuracy allowed a single elemental composition to be obtained for most of the by-products although the mass accuracy threshold was set to 10 ppm. These results are consistent with the theoretical considerations of

Table 1. Possible elemental composition for the unknown $[M-H]^-$ ions calculated by mass accuracy and by spectral accuracy within error of 10 ppm, without atoms constraints ($C \geq 1$, $H \geq 1$, $O \geq 1$, $N \geq 0$, $S \geq 0$) and with $-0.5 \leq DBE \leq 5.0$. The correct match is ranked as number 1 by Spectral accuracy. DBE: double-bond equivalent, RMSE: fit error between the calibrated and theoretical spectrum

By-product number	Measured mass, $[M-H]^- (m/z)$	Elemental composition	Calculated mass (m/z)	Error (ppm)	DBE	Elemental composition	Spectral accuracy	RMSE
1	138.9704	$C_2H_3O_5S^-$	138.9707	-1.9	1.5	$C_2H_3O_5S^-$	95.3373	14
2	140.9860	$C_2H_5O_5S^-$	140.9863	-2.2	0.5	$C_2H_5O_5S^-$	95.4909	8
3	196.9758	$C_4H_5O_7S^-$	196.9761	-1.8	2.5	$C_4H_5O_7S^-$	95.6101	2
4	212.9703	$C_5H_9O_2S_3^-$	196.9770	-6.2	1.5			
		$C_4H_5O_8S^-$	212.9711	-3.6	2.5	$C_4H_5O_8S^-$	96.2591	0
		$CH_5N_6OS_3^-$	212.9692	4.9	2.5	$CH_5N_6OS_3^-$	95.1599	1
5	212.9693	$C_5H_9O_3S_3^-$	212.9719	-7.6	1.5			
		$CH_5N_6OS_3^-$	212.9692	0.3	2.5	$C_4H_5O_8S^-$	98.0143	0
		$C_4H_5O_8S^-$	212.9711	-8.3	2.5		1	
6	224.9733	$C_6H_9O_3S_3^-$	224.9719	6.1	2.5	$C_5H_5O_8S^-$	98.2773	0
		$C_2HN_4O_9^-$	224.9749	-7.1	4.5	$C_2HN_4O_9^-$	95.0093	1
		$C_5H_5O_8S^-$	224.9711	9.9	3.5			
7	224.9732	$C_6H_9O_3S_3^-$	224.9719	5.6	2.5	$C_5H_5O_8S^-$	98.1916	0
		$C_2HN_4O_9^-$	224.9749	7.6	4.5			
		$C_5H_5O_8S^-$	224.9711	9.5	3.5			
8	177.9800	$C_4H_4NO_6S^-$	177.9816	-8.8	3.5	$C_4H_4NO_6S^-$	95.1120	0
9	193.9769	$C_4H_4NO_6S^-$	193.9765	2.1	3.5	$C_4H_4NO_6S^-$	99.0034	0
		$C_5H_8NOS_3^-$	193.9773	-2.3	2.5			
10	193.9749	$C_4H_4NO_6S^-$	193.9765	-8.1	3.5	$C_4H_4NO_6S^-$	99.0130	0
11	115.9978	$C_3H_2NO_4^-$	115.9989	-9.7	3.5	$C_3H_2NO_4^-$	95.4047	1
12	119.9939	$C_2H_2NO_5^-$	119.9938	0.4	2.5	$C_2H_2NO_5^-$	95.0147	1
13	116.9829	$C_3HO_5^-$	116.9829	-0.4	3.5	$C_3HO_5^-$	98.0959	3
14	133.0145	$C_4H_5O_5^-$	133.0142	1.9	2.5	$C_4H_5O_5^-$	98.6007	0
15	149.0100	$C_5H_9OS_2^-$	149.0100	-0.2	1.5	$C_4H_5O_6^-$	98.6302	1
		$C_4H_5O_6^-$	149.0092	5.6	2.5			
16	161.0102	$C_6H_9OS_2^-$	161.0100	1.0	2.5	$C_5H_5O_6^-$	97.9233	0
		$C_5H_5O_6^-$	161.0092	6.4	3.5			
17	179.0196	$C_5H_7O_7^-$	179.0197	-0.7	2.5	$C_5H_7O_7^-$	98.3357	0
		$C_6H_{11}O_2S_2^-$	179.0205	-5.5	1.5			
18	192.9994	$C_5H_5O_8^-$	192.9990	2.1	3.5	$C_5H_5O_8^-$	95.7336	0
		$C_6H_9O_3S_2^-$	192.9998	-2.4	2.5			

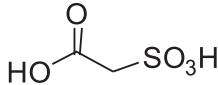
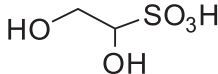
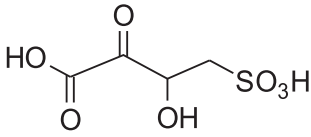
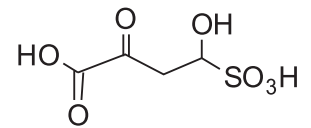
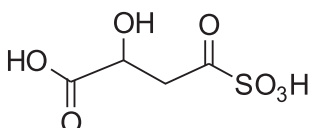
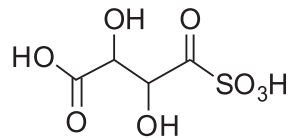
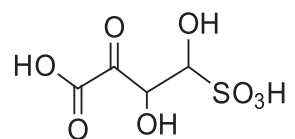
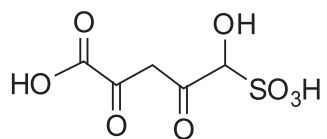
Kind and Fiehn who mentioned that the use of isotopic abundance information (i.e., spectral error) can eliminate 95% of the false candidates.^[42]

The effectiveness of spectral accuracy is particularly evident for by-products 6 and 7 that being isomers both have the elemental composition for their $[M-H]^-$ ions of $C_5H_5O_8S^-$. Specifically, despite their low mass accuracies (9.9 and 9.3 ppm), the observed isotope patterns achieved a spectral accuracy of better than 98%. The above reported elemental composition was associated to their $[M-H]^-$ ions using the same s-CLIPS parameters. The comparison between measured and theoretical isotopic pattern profiles for by-product 6 is reported in Supplementary Fig. S1 (Supporting Information). It should also be noted that although a second possible elemental composition ($C_2HN_4O_9^-$) for the $[M-H]^-$ ion of by-product 6 resulted from the application of spectral accuracy, this was not chemically reasonable due to the low number of hydrogen atoms and high number of oxygen atoms. There was a similar situation for by-product 4 (Table 1) where the second elemental composition obtained employing spectral accuracy was not chemically consistent for an oxidized sulfur-containing compound, as each sulfur atom usually requires at least two oxygen atoms. An excellent result was obtained for by-product 9 at m/z 193.9769 for

which spectral accuracy is able to distinguish between the $[M-H]^-$ ions of two possible compounds with similar absolute mass accuracy error. A spectral accuracy value of 99.0% was assigned to the ion of elemental composition $C_4H_4NO_6S^-$. Once elemental compositions had been obtained the chemical structure of the by-products was assessed by obtaining accurate MS/MS spectra using, as a lock mass, the precursor ion mass obtained in single MS mode. The accurate mass measurements of both the $[M-H]^-$ ions and their main product ions are listed in Table 2.

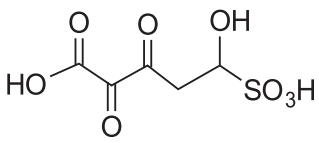
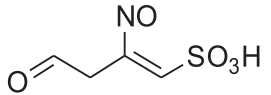
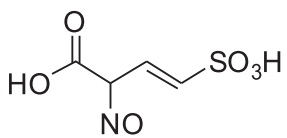
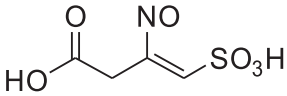
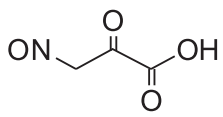
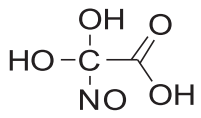
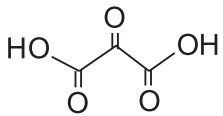
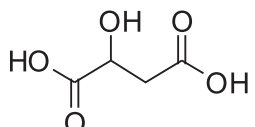
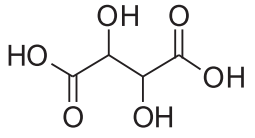
By-products 1 and 2 show $[M-H]^-$ ions at m/z 138.9704 and 140.9860, consistent with the elemental compositions $C_2H_3O_5S^-$ and $C_2H_5O_5S^-$ (errors -1.9 and -2.2 ppm, respectively). Their MS/MS spectra (Figs. 1(a) and 1(b)) show product ions at m/z 79.9563 and 79.9582 for by-products 1 and 2, respectively, which were attributed to the radical anion SO_3^- (errors -13.3 and 10.5 ppm), suggesting that they are sulfur-containing degradation products. Fragmentation of the $[M-H]^-$ ion of by-product 1 also displayed the presence of a carboxylic group in the parent compound due to the product ion at m/z 94.9815 assigned to $CH_3O_3S^-$ (error 6.9 ppm). These experimental results suggested that by-product 1 was a carboxymethanesulfonate, probably formed by further oxidation of the carbonyl group of the

Table 2. Chemical structures of identified by-products, accurate mass measurements and elemental compositions of $[M-H]^-$ ions as well as their product ions detected using IC/QqTOFMS and IC/QqTOFMS/MS analysis. CV: collision voltage

	By-product	Measured $[M-H]^-$ mass (m/z)	CV (V)	Major ions (m/z)	Elemental composition	Calculated mass (m/z)	Error (ppm)	
(1)		138.9704	20	138.9704 94.9815 79.9563	$C_2H_3O_5S^-$ $CH_3O_3S^-$ SO_3^-	138.9707 94.9808 79.9574	-1.9 6.9 -13.3	
(2)		140.9860	20	140.9860 122.9793 94.9816 79.9582	$C_2H_5O_5S^-$ $C_2H_3O_4S^-$ $CH_3O_3S^-$ SO_3^-	140.9863 122.9758 94.9808 79.9574	-2.2 28.8 8.0 10.5	
(3)	A 	196.9758	20	196.9758 178.9585 152.9847 134.9793 80.9661 71.0167	$C_4H_5O_7S^-$ $C_4H_3O_6S^-$ $C_3H_5O_5S^-$ $C_3H_3O_4S^-$ HSO_3^- $C_3H_3O_2^-$	196.9761 178.9656 152.9863 134.9758 80.9652 71.0139	-1.8 -39.6 10.6 26.3 11.3 40.1	
	B 							
	C 							
(4)		212.9703	10	212.9703 168.9782 150.9669 96.9471	$C_4H_5O_8S^-$ $C_3H_5O_6S^-$ $C_3H_3O_5S^-$ HSO_4^-	212.9711 168.9812 150.9707 96.9601	-3.6 -17.9 -25.2 -134	
(5)		212.9693	10	212.9693 168.9832 120.9626	$C_4H_5O_8S^-$ $C_3H_5O_6S^-$ $C_2HO_4S^-$	212.9711 168.9812 120.9601	-8.3 11.6 20.6	
(6)		224.9733	10	224.9733 180.9802 142.9946 110.9784 96.9623	$C_5H_5O_8S^-$ $C_4H_5O_6S^-$ $C_3H_3O_5^-$ $CH_3O_4S^-$ HSO_4^-	224.9711 180.9812 142.9986 110.9758 96.9601	9.9 -5.7 -27.9 23.8 22.7	

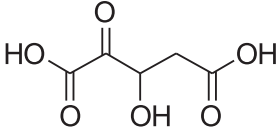
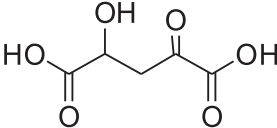
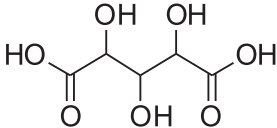
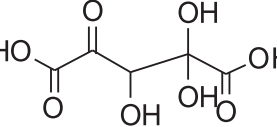
(Continues)

Table 2. (Continued)

	By-product	Measured [M-H] ⁻ mass (<i>m/z</i>)	CV (V)	Major ions (<i>m/z</i>)	Elemental composition	Calculated mass (<i>m/z</i>)	Error (ppm)
(7)		224.9732	10	224.9732	C ₅ H ₅ O ₈ S ⁻	224.9711	9.5
				152.9861	C ₃ H ₅ O ₅ S ⁻	152.9863	-1.4
				145.0146	C ₅ H ₅ O ₅ ⁻	145.0142	2.4
				134.9774	C ₃ H ₃ O ₄ S ⁻	134.9758	12.2
				110.9770	CH ₃ O ₄ S ⁻	110.9758	11.2
				106.9830	C ₂ H ₃ O ₃ S ⁻	106.9808	20.2
(8)		177.9800	20	177.9800	C ₄ H ₄ NO ₅ S ⁻	177.9816	-8.8
				159.9744	C ₄ H ₂ NO ₄ S ⁻	159.9710	21.2
				96.0104	C ₄ H ₂ NO ₂ ⁻	96.0091	13.5
				80.9668	HSO ₃ ⁻	80.9652	19.9
(9)		193.9769	20	193.9769	C ₄ H ₄ NO ₆ S ⁻	193.9765	2.1
				149.9865	C ₃ H ₄ NO ₄ S ⁻	149.9867	-1.0
				113.0090	C ₄ H ₃ NO ₃ ⁻	113.0118	-25.1
				106.9815	C ₂ H ₃ O ₃ S ⁻	106.9808	6.2
				80.9637	HSO ₃ ⁻	80.9651	-18.4
(10)		193.9749	20	193.9749	C ₄ H ₄ NO ₆ S ⁻	193.9765	-8.1
				175.9639	C ₄ H ₂ NO ₅ S ⁻	175.9659	-11.5
				119.9876	C ₃ H ₄ O ₃ S ⁻	119.9887	-8.9
				112.0060	C ₄ H ₂ NO ₃ ⁻	112.004	17.7
				80.9648	HSO ₃ ⁻	80.9652	-4.8
(11)		115.9978	20	115.9975	C ₃ H ₂ NO ₄ ⁻	115.9989	-9.7
				72.0099	C ₂ H ₂ NO ₂ ⁻	72.0091	11.1
(12)		119.9939	20	119.9939	C ₂ H ₂ NO ₅ ⁻	119.9938	0.4
				89.9968	C ₂ H ₂ O ₄ ⁻	89.9959	10.5
(13)		116.9829	10	116.9829	C ₃ HO ₅ ⁻	116.9829	-0.4
				72.9906	C ₂ HO ₃ ⁻	72.9931	-34.5
(14)		133.0145	20	133.0145	C ₄ H ₅ O ₅ ⁻	133.0142	-1.9
				115.0026	C ₄ H ₃ O ₄ ⁻	115.0037	-9.4
				89.0247	C ₃ H ₅ O ₃ ⁻	89.0244	3.2
				72.9931	C ₂ HO ₃ ⁻	72.9931	-0.2
				71.0142	C ₃ H ₃ O ₂ ⁻	71.0139	4.9
				59.0144	C ₂ H ₃ O ₂ ⁻	59.0139	9.3
(15)		149.0100	20	149.0100	C ₄ H ₅ O ₆ ⁻	149.0092	5.6
				130.9991	C ₄ H ₃ O ₅ ⁻	130.9986	3.8
				105.0185	C ₃ H ₅ O ₄ ⁻	105.0193	-7.9
				87.0078	C ₃ H ₃ O ₃ ⁻	87.0088	-11.1

(Continues)

Table 2. (Continued)

By-product	Measured [M-H] ⁻ mass (<i>m/z</i>)	CV (V)	Major ions (<i>m/z</i>)	Elemental composition	Calculated mass (<i>m/z</i>)	Error (ppm)
(16) A 	161.0102	20	161.0102	C ₅ H ₅ O ₆ ⁻	161.0092	-6.4
			142.9980	C ₅ H ₃ O ₅ ⁻	142.9986	-4.2
			117.0191	C ₄ H ₅ O ₄ ⁻	117.0193	-2.0
			99.0093	C ₄ H ₃ O ₃ ⁻	99.0088	5.4
(17) B 	179.0196	20	179.0196	C ₅ H ₇ O ₇ ⁻	179.0197	-0.7
			161.0095	C ₅ H ₅ O ₆ ⁻	161.0092	2.1
(18) 	192.9994	20	133.0142	C ₄ H ₅ O ₅ ⁻	133.0142	-0.3
			103.0028	C ₃ H ₃ O ₄ ⁻	103.0037	-8.6
			99.0078	C ₄ H ₃ O ₃ ⁻	99.0088	-9.8
			89.0234	C ₃ H ₅ O ₃ ⁻	89.0244	-11.4
			71.0128	C ₃ H ₃ O ₂ ⁻	71.0139	-15.5
			59.0126	C ₂ H ₃ O ₂ ⁻	59.0139	-21.2
(18) 	192.9994	20	192.9994	C ₅ H ₅ O ₈ ⁻	192.9990	2.1
			149.0094	C ₄ H ₅ O ₆ ⁻	149.0092	1.6
			121.0140	C ₃ H ₅ O ₅ ⁻	121.0142	-2.0
			105.0190	C ₃ H ₅ O ₄ ⁻	105.0193	-3.2
			77.0236	C ₂ H ₅ O ₃ ⁻	77.0244	-10.6

previously detected 2-oxoethanesulfonic acid.^[14] The product ion mass spectrum of deprotonated by-product 2 (Fig. 1(b)) revealed an ion at *m/z* 122.9793 with elemental composition of C₂H₃O₄S⁻. It was formed through loss of water from the [M-H]⁻ ion, indicating the probable presence of a hydroxyl group in by-product 2. This compound was a 1,2-dihydroxyethanesulfonate, formed by cleavage of the Uniblu-OH 2-hydroxyethylsulfonyl group and hydroxylation at the 1-position. All the information obtained from the product ion spectra of by-products 1 and 2 is rationalized in the fragmentation pathways depicted in Supplementary Fig. S2 (Supporting Information) and Fig. 2, respectively.

By-product 3 showed a [M-H]⁻ ion at *m/z* 196.9758 consistent with elemental composition C₄H₅O₇S⁻ (error -1.8 ppm) for which three possible chemical structures can be proposed (Table 2). Its product ion mass spectrum (Supplementary Fig. S3, Supporting Information) revealed an ion at *m/z* 80.9661 attributed to HSO₃⁻ (error 11.3 ppm) suggesting this compound to be another sulfur-containing by-product. Examination of the product ion spectrum reveals other minor ions at *m/z* 178.9585, 152.9847 and 134.9793 with elemental compositions C₄H₃O₆S⁻, C₃H₅O₅S⁻ and C₃H₃O₄S⁻, respectively. The first two ions can be rationalized through loss of water and carbon dioxide from the precursor ion, respectively. Both these product ions led to the formation of the third product ion (*m/z* 134.9793) through

further loss of CO₂ and water, respectively. Finally, a product ion at *m/z* 71.0167, assigned to C₃H₃O₂⁻ (error 40.1 ppm), can be rationalized by loss of sulfurous acid from the above discussed product ion at *m/z* 153. The high errors associated with some of the product ions of by-product 3 are reasonable, due to their low signal intensity. The product ion spectrum of deprotonated by-product 3 did not allow us to unequivocally assign its structure, there being three possible structures: 3-carboxy-3-oxopropane-1-sulfonate, substituted with a hydroxyl group at position 1 (A) or 2 (B) and 3-carboxy-3-hydroxy-1-oxopropane-1-sulfonate (C). All three structures are consistent with the fragmentation pattern outlined in Supplementary Fig. S4 (Supporting Information).

By-products 4 and 5 are two closely eluting isomers having [M-H]⁻ ions at *m/z* 212.9703 and 212.9693. On the basis of both spectral accuracy (Table 1) and mass accuracy (Table 2), their elemental composition was assigned as C₄H₅O₈S⁻ (errors -3.6 and -8.3 ppm, respectively) suggesting that these by-products were the result of a hydroxylation on by-product 3. Interestingly, the product ion spectrum of deprotonated by-product 5 (Table 2) showed a diagnostic ion at *m/z* 120.9626, not observed for by-product 4, with elemental composition of C₂HO₄S⁻ (error 20.6 ppm). Its formation was rationalized by consecutive loss of water and formaldehyde from the ion at *m/z* 168.9832 assigned to C₃H₅O₆S⁻ (error 11.6 ppm). This

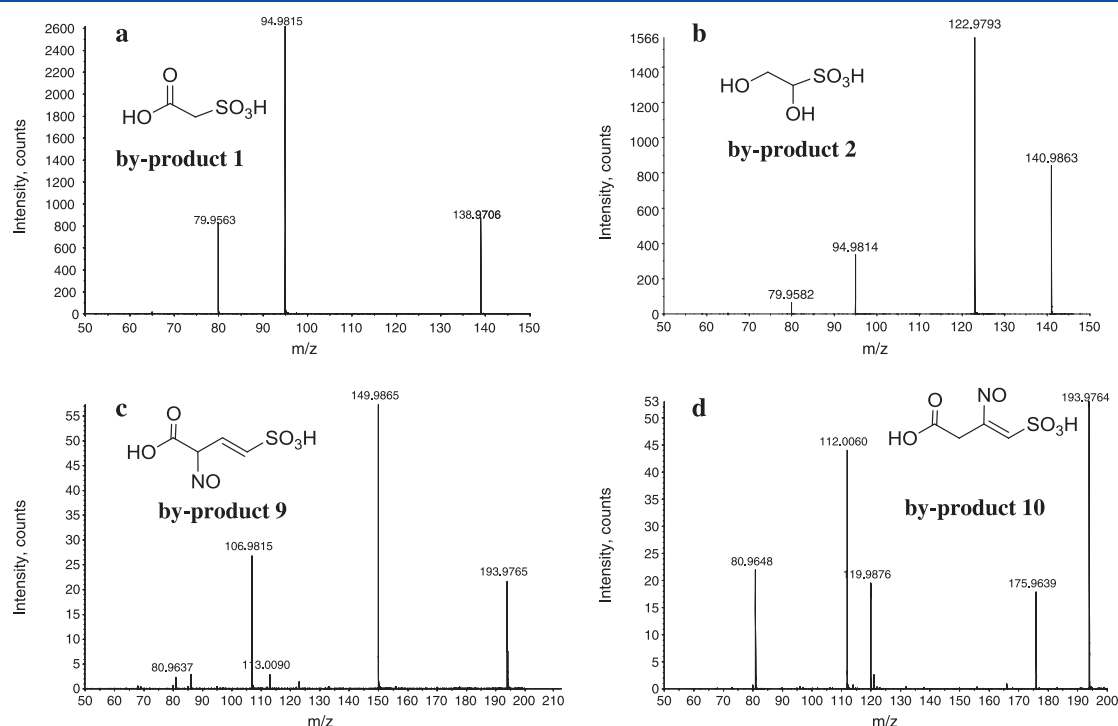


Figure 1. Calibrated product ion spectra of $[M-H]^-$ ions of (a) by-product 1, (b) by-product 2, (c) by-product 9, and (d) by-product 10. $[M-H]^-$ ions at m/z 138.9707, 140.9863 and 193.9765 were used as lock masses. CV = 20 V.

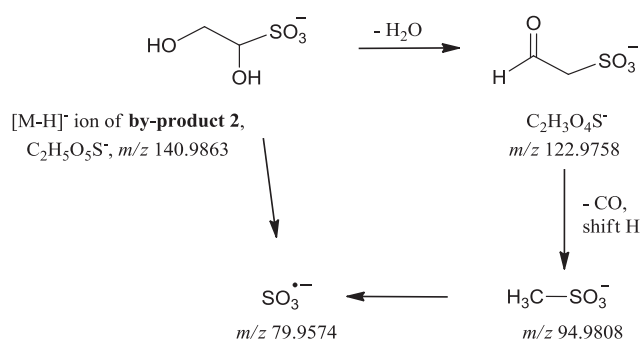


Figure 2. Proposed fragmentation pathway of $[M-H]^-$ ion of by-product 2 from IC/QqTOFMS/MS data at CV = 20 V. Accurate mass measurements of product ions are reported in Table 2.

finding led to by-product 5 being unequivocally assigned as 3-carboxy-1,2-dihydroxy-3-oxopropane-1-sulfonate. The structure of by-product 4 was proposed to be 3-carboxy-2,3-dihydroxy-1-oxopropane-1-sulfonate. The identified product ions of these structures were consistent with the fragmentation patterns outlined in Supplementary Figs. S5 and S6 (Supporting Information).

By-products 6 and 7 were two closely eluting isomers, which showed $[M-H]^-$ ions at m/z 224.9733 and 224.9732. The elemental composition of both ions was determined to be $C_5H_5O_8S^-$ based on mass accuracy (errors -9.9 and -9.5 ppm, respectively) and spectral accuracy (Table 2). Their fragmentation patterns showed significant differences, allowing the different chemical structures to be determined. Both

compounds were sulfur-containing by-products as demonstrated by the presence of product ions at m/z 96.9623 and 96.9579 assigned to HSO_4^- (errors 22.7 and -22.7 ppm, respectively). The ions at m/z 110.9784 and 110.9770 were consistent with the elemental composition $CH_3O_4S^-$ (errors 23.8 and 11.2 ppm, respectively). The presence of such a product ion made it probable that both compounds had a hydroxyl group at the α -position of the sulfur group. Two other ions in the product ion spectrum of deprotonated by-product 6 (Supplementary Fig. S7(a), Supporting Information) at m/z 180.9892 and 142.9946 with elemental compositions $C_4H_5O_6S^-$ and $C_5H_3O_5^-$ (errors -5.7 and -27.9 ppm, respectively) suggested neutral loss of CO_2 and H_2SO_3 , respectively, from the $[M-H]^-$ ion. The product ion spectrum of deprotonated by-product 7 (Supplementary Fig. S7(b), Supporting Information) showed a base peak at m/z 152.9861 with elemental composition $C_3H_5O_5S^-$ (error -1.4 ppm) probably arising from homolytic carbon-carbon cleavage between the carbonyl groups in positions 3 and 4 of the $[M-H]^-$ ion. This product ion, in turn, gave rise to ions at m/z 134.9774 and then at m/z 106.9830 through consecutive losses of water and CO. On the basis of the identified product ions of deprotonated by-products 6 and 7, the fragmentation patterns outlined in Supplementary Figs. S7(c) and S7(d) (Supporting Information) were proposed.

By-products 8–12 all showed even-mass $[M-H]^-$ ions suggesting that they were nitrogen-containing compounds. The product ion spectra of deprotonated by-products 8–10 revealed the presence of an ion at m/z 81 whose accurate mass was consistent with the elemental composition HSO_3^- , as already found for by-product 3. By-products 9 and 10 showed $[M-H]^-$ ions with the same elemental composition of

$C_4H_4NO_6S^-$ (errors 2.1 and -8.1 ppm, respectively). However, the fragmentation patterns of these ions showed significant differences (Figs. 2(c) and 2(d)). Specifically, the product ion spectrum of deprotonated by-product 9 showed a base peak at m/z 149.9865 with elemental composition $C_3H_4NO_4S^-$ (error -1.0 ppm). This is consistent with CO_2 loss, indicating the presence of a monocarboxylic acid group. A close examination of this product ion spectrum revealed another minor odd-electron ion at m/z 113.0090, corresponding to the radical ion with an elemental composition of $C_4H_3NO_3^-$, which derives from elimination of the HSO_3^- radical ion from the $[M-H]^-$ ion. This by-product was assigned as 3-carboxy-3-nitrosoprop-1-ene-1-sulfonate. The product ion mass spectrum of deprotonated by-product 10 revealed an ion at m/z 175.9639 and an odd-electron ion at m/z 119.9876, consistent with elemental compositions $C_4H_2NO_5S^-$ and $C_3H_4O_3S^-$ (errors -11.5 and -8.9 ppm), respectively. The former ion was derived through the loss of water, while the latter derived from consecutive elimination of carbon dioxide and an NO radical. Both these product ions suggest the presence of a monocarboxylic acid. In addition, the base peak of the product ion spectrum was at m/z 112.0060 with elemental composition $C_4H_2NO_3^-$ (error 17.7 ppm) probably arising from loss of H_2SO_3 from the $[M-H]^-$ ion and further migration of the NO group to the terminal carbon. The structure was thus assigned as 3-carboxy-3-nitrosoprop-1-ene-2-sulfonate, with the nitro group probably located at the β -position of the carboxylic acid group. This compound can

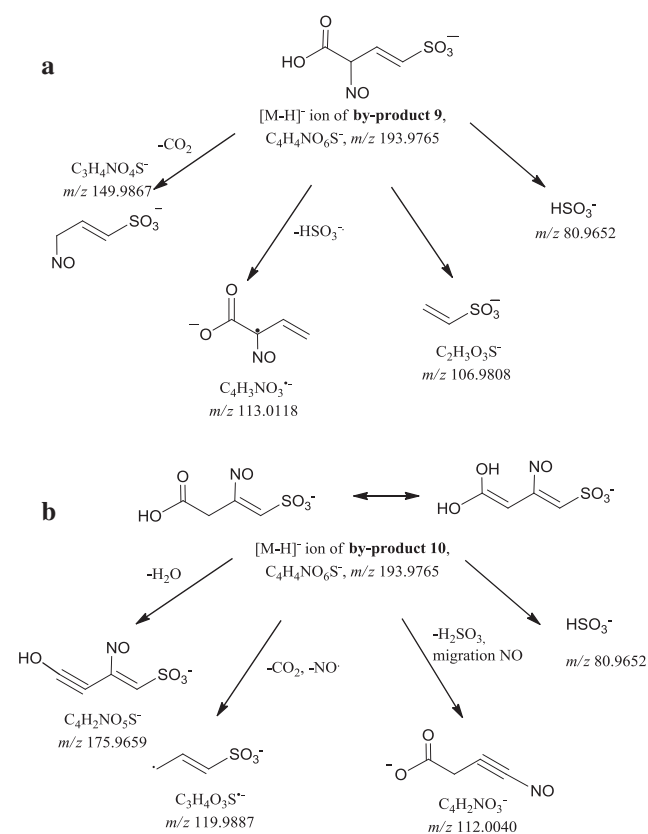


Figure 3. Proposed fragmentation pathway of $[M-H]^-$ ions of by-product 9 (a) and 10 (b) from IC/QqTOFMS/MS data at $CV=20$ V. Accurate mass measurements of product ions are reported in Table 2.

be correlated with by-product 8 by a further oxidation of the terminal carbon. Based on the identified product ions of by-products 9 and 10 the fragmentation patterns outlined in Figs. 3(a) and 3(b) were proposed.

Table 1 also shows that by-products 13–18 yielded product ions consistent with consecutive neutral loss of 44 and 18 Da, indicating the presence of a carboxylic acid and a hydroxyl group, respectively. Therefore, the structures of these compounds were consistent with mono- and polyhydroxylated dicarboxylic acids of low molecular weight. By-product 13 with its $[M-H]^-$ ion at m/z 116.9829, assigned to $C_3HO_5^-$ (error -0.4 ppm), was previously identified as the corresponding DPNH derivative, derivatized at the oxo position.^[14] By-product 14 showed a $[M-H]^-$ ion at m/z 133.0145 with elemental composition $C_4H_5O_5^-$ (error -1.9 ppm) whose product ion spectrum (Fig. 4) showed an intense ion at m/z 115.0026 and a minor one at m/z 89.0247 with elemental compositions $C_4H_3O_4^-$ and $C_3H_5O_3^-$ (errors -9.4 and 3.2 ppm, respectively). These ions were formed by competitive loss of water and CO_2 , respectively, and both underwent further fragmentation leading to acrylate and acetate ions through CO_2 and formaldehyde loss. In addition, the ion at m/z 72.9931, assigned to deprotonated glyoxylic acid (error -0.2 ppm), could be rationalized by $C_2H_4O_2$ loss through cleavage at the 2-3 position on the $[M-H]^-$ ion. This information allowed us to assign by-product 14 to 2-hydroxysuccinic acid whose fragmentation pathway is depicted in Fig. 5. On the basis of exact mass measurement data, and confirmed by high spectral accuracy (better than 98%), by-products 15–17 were assigned as listed in Table 2. In particular, by-product 15 showed a $[M-H]^-$ ion at m/z 149.0100 with elemental composition $C_4H_5O_6^-$ (error 5.6 ppm), consistent with the conjugated form of 2,3-dihydroxysuccinic acid. This suggested that the compound was formed by a further hydroxylation of by-product 14. The product ion spectrum of deprotonated by-product 16 did not allow us to distinguish between two possible dicarboxylic acid structures: 3-hydroxy-2-oxopentanedioic acid and 2-hydroxy-4-oxopentanedioic acid. By-product 17 showed a $[M-H]^-$ ion at m/z 179.0196 with elemental composition $C_5H_7O_7^-$ (error -0.7 ppm), assigned as deprotonated 2,3,4-trihydroxypentanedioic acid.

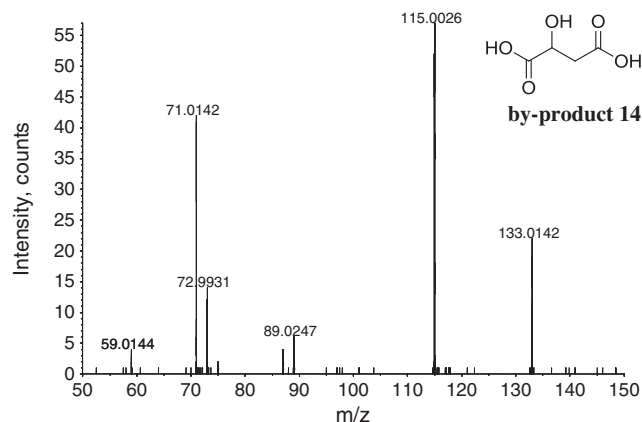


Figure 4. Calibrated product ion spectrum of $[M-H]^-$ ion of by-product 14 at $CV=20$ V. $[M-H]^-$ ion at m/z 133.0142 was used as a lock mass.

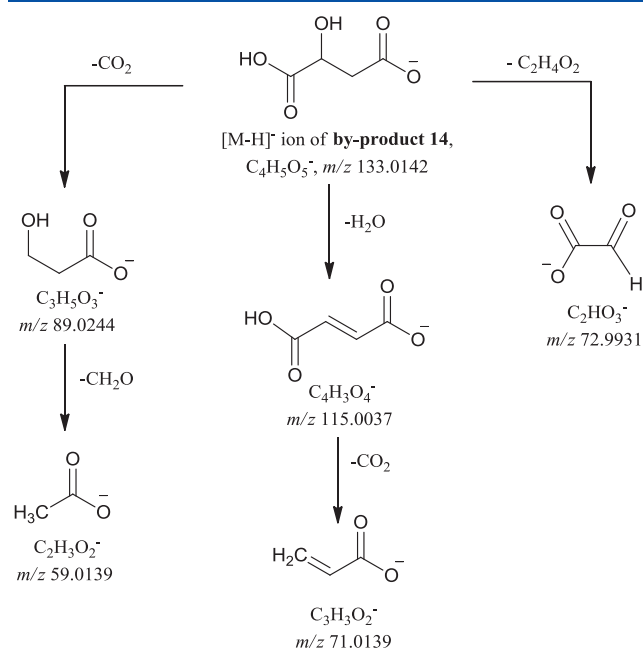


Figure 5. Proposed fragmentation pathway of $[M-H]^-$ ion of by-product 14 from IC/QqTOFMS/MS data at CV = 20 V. Accurate mass measurements of product ions are reported in Table 2.

The last identified compound, by-product 18, showed a $[M-H]^-$ ion at m/z 192.9994, with elemental composition $C_5H_5O_8^-$ (error 2.1 ppm), whose product ion spectrum (Supplementary Fig. S8, Supporting Information) showed major ions at m/z 149.0094 and 105.0190 with elemental compositions $C_4H_5O_6^-$ and $C_3H_5O_4^-$ (errors 1.6 and -3.2 ppm, respectively). These ions were formed by consecutive losses of CO_2 from the $[M-H]^-$ ion, indicating that this by-product was a dicarboxylic acid. A product ion at m/z 121.0140 of elemental composition $C_3H_5O_5^-$ (error -2.0 ppm) was derived by CO elimination from m/z 149. This finding allowed the oxo group to be located at the 4-position. The structure of this compound was assigned as 2,2,3-trihydroxy-4-oxopentanedioic acid. Interestingly, the absence of any water loss in the product ion spectrum could be explained by the fact that all positions on the aliphatic chain are locked and thus the dehydration pathway was not possible. The information obtained from the product ion spectrum was rationalized in the fragmentation pathway depicted in Supplementary Fig. S9 (Supporting Information).

Formation mechanism of identified low molecular weight organic acids

The formation/degradation of identified organic acids was monitored over a long ozonation time in order to gain insights into their formation mechanism, and selected measured profiles are depicted in Fig. 6. The identified by-products were consistent with further oxidation and decarboxylation of the previously identified carbonyl by-products.^[14] From Fig. 6 it can be seen that by-product 12 was always formed at ozonation times longer than 90 min, suggesting that it was an end by-product. A careful analysis of the measured profiles shown in Fig. 6, including possible structures of low molecular weight carboxylic acids

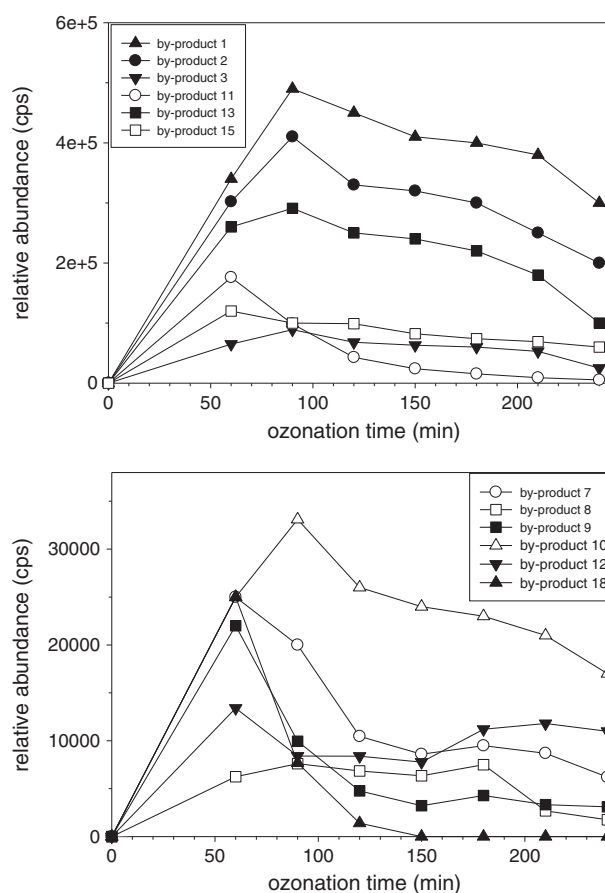


Figure 6. Formation/degradation profiles of selected identified carboxylic acids (extracted ion peak area from IC/ESI-QqTOFMS) during ozonation of Uniblu-OH.

identified over a long ozonation time, could help in understanding the reaction pathway depicted in Fig. 7. The identified organic acids (Table 1) arose from further degradation of low molecular weight carbonyl compounds, namely keto-acids and aliphatic aldehydes detected in the early stage of the ozonation process.^[14] Although complex competitive and consecutive reactions occurred during ozonation, it was possible to describe a degradation pathway on the basis of reasonable chemistry, supported by some observed correlations between the by-products belonging to the same class. After the formation of the sulfur-containing by-products 1–7 and by-products 16 and 17, the degradation proceeded further with the decarboxylation of by-product 16 (A) and 16 (B) followed by oxidation of the terminal carbon of the formed intermediate, leading to by-product 14. This oxidation process was based on hydrogen homolytic abstraction by a hydroxyl radical leading to a peroxy radical which, in turn, was transformed into a hydroperoxide. By-product 13 was formed from by-product 17 by means of the same oxidation route. It followed that three of the detected by-products all led to the formation of a single compound, 2-oxomalonic acid (by-product 13). This was also consistent with the formation/decomposition profiles of the detected by-products. By-product 13 was the lowest molecular weight dicarboxylic acid detected and it persisted in high abundance at long reaction times (Fig. 6). The finding that 2-oxomalonic acid slowly disappeared at longer ozonation time suggested that it was

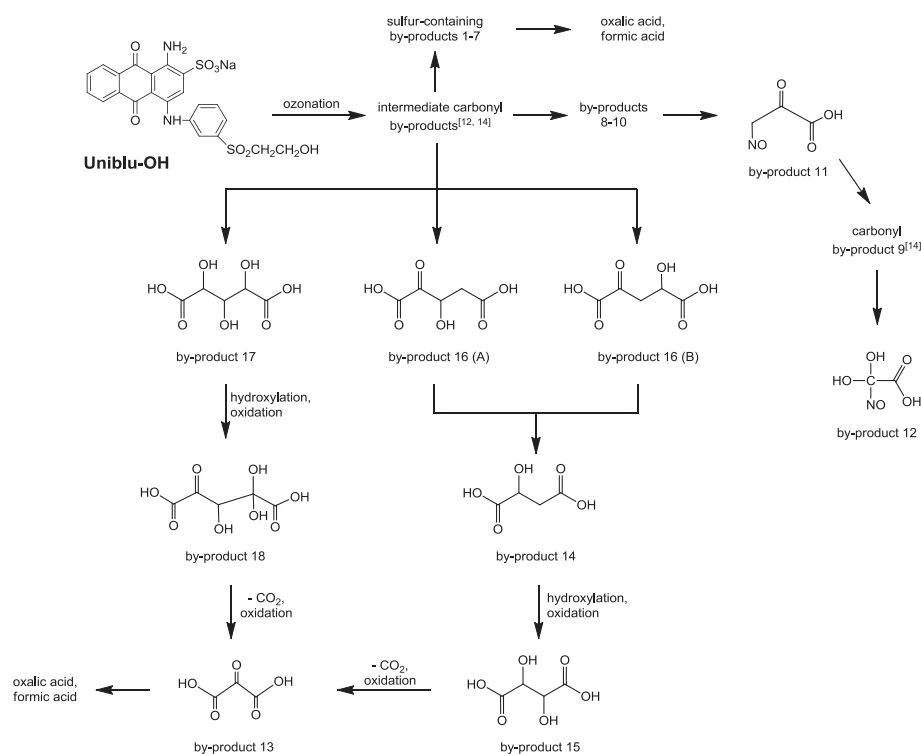


Figure 7. Proposed degradation pathway for Uniblu-OH ozonation leading to low molecular weight organic acids.

degraded to oxalic and/or formic acid, according to previous investigation employing authentic standards.^[12] The same aforementioned mechanisms including decarboxylation and subsequent oxidation can be applied to all the sulfur- and nitrogen-containing by-products 1–12 in order to explain the formation of their lower molecular weight homologues. Sulfur-containing by-products were still persistent at longer ozonation time confirming that the sulfur present in Uniblu-OH did not undergo complete mineralization. Finally, by-product 12 was still formed at longer ozonation time (Fig. 6) and therefore was another end product. This confirmed the finding that the organic nitrogen compound, Uniblu-OH, was not completely mineralized.

CONCLUSIONS

The coupling of ion chromatography (IC) and electrospray ionization mass spectrometry (ESI-MS), proved to be a powerful technique for the identification of low molecular weight organic acids formed as final by-products of Uniblu-OH degradation by the ozonation process, an oxidation method widely employed to degrade recalcitrant organic pollutants in industrial wastewater. Organic acid identification was possible due to the employment of a NaOH gradient and a membrane ion suppressor that minimized the background spectral interferences and enhanced the signals of the $[M-H]^-$ ions. The combination of mass accuracy, MS/MS information and high spectral accuracy was demonstrated to be a powerful method for unequivocally assigning a single chemical composition to each identified compound. Specifically, the employment of the spectral accuracy concept using

the sCLIPS algorithm allowed the unequivocal identification of 18 low molecular weight organic acids as a result of extensive oxidation of the parent organic pollutant. Excellent spectral accuracy of better than or close to 95% was found for most of the identified compounds. Most of the by-products gave rise in the MS collision cell to either single or double CO_2 and water loss, consistent with assignment to polyhydroxylated carboxylic acids. Some of identified organic acids were shown to be both sulfur- and nitrogen-containing carbonyl by-products. Due to the complexity of reactions involved during Uniblu-OH ozonation it was possible to assess the presence of correlations between different identified by-products, such as polyhydroxylated carboxylic acids. These compounds in turn decompose to known low molecular weight organic acids through decarboxylation and further oxidation and then undergo complete mineralization. However, sulfur- and nitrogen-containing compounds still remain at longer ozonation times. This result is of environmental interest due to the potential toxicity of such compounds.

SUPPORTING INFORMATION

Additional supporting information may be found in the online version of this article.

Acknowledgements

This work was partially supported by Apulia Region by funding from the Rela-Valbior Project within the Scientific Research Framework Program 2007-2013.

REFERENCES

- [1] A. Lopez, C. Di Iaconi, G. Mascolo, A. Pollice, in *Innovative and Integrated Technologies for the Treatment of Industrial Wastewater (INNOWATECH)*, IWA Publishing, 2011.
- [2] P. R. Gogate, A. B. Pandit. A review of imperative technologies for wastewater treatment II: hybrid methods. *Adv. Environ. Res.* **2004**, *8*, 553.
- [3] M. Pera-Titus, V. Garcia-Molina, M. A. Baños, J. Giménez, S. Esplugas. Degradation of chlorophenols by means of advanced oxidation processes: a general review. *Appl. Catal. B Environ.* **2004**, *47*, 219.
- [4] S. Devipriya, S. Yesodharan. Photocatalytic degradation of pesticide contaminants in water. *Solar Energy Materials and Solar Cells* **2005**, *86*, 309.
- [5] J. J. Pignatello, E. Oliveros, A. MacKay. Advanced oxidation processes for organic contaminant destruction based on the Fenton reaction and related chemistry. *Crit. Rev. Environ. Sci. Technol.* **2006**, *36*, 1.
- [6] C. Comninellis, A. Kapalka, S. Malato, S. A. Parsons, I. Poullos, D. Mantzavinos. Advanced oxidation processes for water treatment: advances and trends for R&D. *J. Chem. Technol. Biotechnol.* **2008**, *83*, 769.
- [7] M. A. Shannon, P. W. Bohn, M. Elimelech, J. G. Georgiadis, B. J. Marinas, A. M. Mayes. Science and technology for water purification in the coming decades. *Nature* **2008**, *452*, 301.
- [8] L. Rizzo. Bioassays as a tool for evaluating advanced oxidation processes in water and wastewater treatment. *Water Res.* **2011**, *45*, 4311.
- [9] S. Malato, P. Fernández-Ibáñez, M. I. Maldonado, J. Blanco, W. Gernjak. Decontamination and disinfection of water by solar photocatalysis: Recent overview and trends. *Catal. Today* **2009**, *147*, 1.
- [10] M. Constapel, M. Schellenträger, J. M. Marzinkowski, S. Gäb. Degradation of reactive dyes in wastewater from the textile industry by ozone: Analysis of the products by accurate masses. *Water Res.* **2009**, *43*, 733.
- [11] A. Detomaso, G. Mascolo, A. Lopez. Characterization of carbofuran photodegradation by-products by liquid chromatography/hybrid quadrupole time-of-flight mass spectrometry. *Rapid Commun. Mass Spectrom.* **2005**, *19*, 2193.
- [12] G. Mascolo, A. Lopez, A. Bozzi, G. Tiravanti. By-products formation during the ozonation of the reactive dye Uniblu-A. *Ozone-Sci. Eng.* **2002**, *24*, 439.
- [13] D. Deng, J. Guo, G. Zeng, G. Sun. Decolorization of anthraquinone, triphenylmethane and azo dyes by a new isolated *Bacillus cereus* strain DC11. *Int. Biodeter. Biodegr.* **2008**, *62*, 263.
- [14] A. Amorisco, V. Locaputo, G. Mascolo. Characterization of carbonyl by-products during Uniblu-A ozonation by liquid chromatography/hybrid quadrupole time-of-flight mass spectrometry. *Rapid Commun. Mass Spectrom.* **2011**, *25*, 1801.
- [15] J. A. Cruwys, R. M. Dinsdale, F. R. Hawkes, D. L. Hawkes. Development of a static headspace gas chromatographic procedure for the routine analysis of volatile fatty acids in wastewaters. *J. Chromatogr. A* **2002**, *945*, 195.
- [16] W.-J. Huang, G.-C. Fang, C.-C. Wang. The determination and fate of disinfection by-products from ozonation of polluted raw water. *Sci. Total Environ.* **2005**, *345*, 261.
- [17] J. Chen, B. P. Preston, M. J. Zimmerman. Analysis of organic acids in industrial samples comparison of capillary electrophoresis and ion chromatography. *J. Chromatogr. A* **1997**, *781*, 205.
- [18] Y. Deng, X. Fan, A. Delgado, C. Nolan, K. Furton, Y. Zuo, R. D. Jones. Separation and determination of aromatic acids in natural water with preconcentration by capillary zone electrophoresis. *J. Chromatogr. A* **1998**, *817*, 145.
- [19] S. Uchiyama, E. Matsushima, S. Aoyagi, M. Ando. Simultaneous determination of C1–C4 carboxylic acids and aldehydes using 2,4-dinitrophenylhydrazine-impregnated silica gel and high-performance liquid chromatography. *Anal. Chem.* **2004**, *76*, 5849.
- [20] S.-F. Chen, R. A. Mowery, V. A. Castleberry, G. P. v. Walsum, C. K. Chambliss. High-performance liquid chromatography method for simultaneous determination of aliphatic acid, aromatic acid and neutral degradation products in biomass pretreatment hydrolysates. *J. Chromatogr. A* **2006**, *1104*, 54.
- [21] K. Fischer. Environmental analysis of aliphatic carboxylic acids by ion-exclusion chromatography. *Anal. Chim. Acta* **2002**, *465*, 157.
- [22] K. Ohta, M. Ohashi, J.-Y. Jin, T. Takeuchi, C. Fujimoto, S.-H. Choi, J. J. Ryoo, K.-P. Lee. Retention behavior of C1–C6 aliphatic monoamines on anion-exchange and polymethacrylate resins with heptylamine as eluent. *J. Chromatogr. A* **2004**, *1039*, 179.
- [23] M. C. Bruzzoniti, E. Mentasti, C. Sarzanini, P. Hajós. Ion chromatographic separation of carboxylic acids prediction of retention data. *J. Chromatogr. A* **1997**, *770*, 13.
- [24] S. A. Cassidy, C. W. Demarest, P. B. Wright, J. B. Zimmerman. Development and application of a universal method for quantitation of anionic constituents in active pharmaceutical ingredients during early development using suppressed conductivity ion chromatography. *J. Pharm. Biomed. Anal.* **2004**, *34*, 255.
- [25] J. Qiu, X. Jin. Development and optimization of organic acid analysis in tobacco with ion chromatography and suppressed conductivity detection. *J. Chromatogr. A* **2002**, *950*, 81.
- [26] K.-H. Bauer, T. P. Knepper, A. Maes, V. Schatz, M. Voihsel. Analysis of polar organic micropollutants in water with ion chromatography–electrospray mass spectrometry. *J. Chromatogr. A* **1999**, *837*, 117.
- [27] L. Charles, D. Pépin, B. Casetta. Electrospray ion chromatography – tandem mass spectrometry of bromate at sub-ppb levels in water. *Anal. Chem.* **1996**, *68*, 2554.
- [28] K. Gamoh, H. Saitoh, H. Wada. Improved liquid chromatography/mass spectrometric analysis of low molecular weight carboxylic acids by ion exclusion separation with electrospray ionization. *Rapid Commun. Mass Spectrom.* **2003**, *17*, 685.
- [29] S. B. Mohsin. Ion chromatography coupled with mass spectrometry for the determination of ionic compounds in agricultural chemicals. *Anal. Chem.* **1999**, *71*, 3603.
- [30] M. I. H. Helaleh, K. Tanaka, H. Taoda, W. Hu, K. Hasebe, P. R. Haddad. Qualitative analysis of some carboxylic acids by ion-exclusion chromatography with atmospheric pressure chemical ionization mass spectrometric detection. *J. Chromatogr. A* **2002**, *956*, 201.
- [31] R. Roehl, R. Slingsby, N. Avdalovic, P. E. Jackson. Applications of ion chromatography with electrospray mass spectrometric detection to the determination of environmental contaminants in water. *J. Chromatogr. A* **2002**, *956*, 245.
- [32] J. M. Käkölä, R. J. Alén, J. P. Isoaho, R. B. Matilainen. Determination of low-molecular-mass aliphatic carboxylic acids and inorganic anions from kraft black liquors by ion chromatography. *J. Chromatogr. A* **2008**, *1190*, 150.
- [33] X. Xiang, C. Y. Ko, H. Y. Guh. Ion-exchange chromatography/electrospray mass spectrometry for the identification of organic and inorganic species in topiramate tablets. *Anal. Chem.* **1996**, *68*, 3726.
- [34] G. Mascolo, A. Lopez, A. Detomaso, G. Lovecchio. Ion chromatography–electrospray mass spectrometry for the identification of low-molecular-weight organic acids during the 2,4-dichlorophenol degradation. *J. Chromatogr. A* **2005**, *1067*, 191.

- [35] W. Buchberger, W. Ahrer. Combination of suppressed and non-suppressed ion chromatography with atmospheric pressure ionization mass spectrometry for the determination of anions. *J. Chromatogr. A* **1999**, *850*, 99.
- [36] W. W. Buchberger. Detection techniques in ion analysis: what are our choices? *J. Chromatogr. A* **2000**, *884*, 3.
- [37] W. Jiang, J. C. L. Erve. Spectral accuracy of a new hybrid quadrupole time-of-flight mass spectrometer: application to ranking small molecule elemental compositions. *Rapid Commun. Mass Spectrom.* **2012**, *26*, 1014.
- [38] Y. Wang, M. Gu. The concept of spectral accuracy for MS. *Anal. Chem.* **2010**, *82*, 7055.
- [39] A. L. Rockwood, S. L. Van Orden. Ultrahigh-speed calculation of isotope distributions. *Anal. Chem.* **1996**, *68*, 2027.
- [40] A. L. Rockwood, S. L. Van Orden, R. D. Smith. Ultrahigh resolution isotope distribution calculations. *Rapid Commun. Mass Spectrom.* **1996**, *10*, 54.
- [41] J. A. Yergey. A general approach to calculating isotopic distributions for mass spectrometry. *Int. J. Mass Spectrom. Ion Phys.* **1983**, *52*, 337.
- [42] T. Kind, O. Fiehn. Seven Golden Rules for heuristic filtering of molecular formulas obtained by accurate mass spectrometry. *BMC Bioinformatics* **2007**, *8*, 105.